

On the viscous steady flow around a circular cylinder

F. Mandujano and R. Peralta-Fabi

*Departamento de Física, Facultad de Ciencias, Universidad Nacional Autónoma de México,
e-mail: paco@graef.fciencias.unam.mx, rpfabi@hp.fciencias.unam.mx*

Recibido el 16 de agosto de 2004; aceptado el 22 de noviembre de 2004

A series truncation method is proposed to obtain approximate solutions to the flow past a circular cylinder. This procedure is based on a change in the radial coordinate (x), such that this new coordinate is defined in a finite interval. Solutions are truncated power series in x , so that the full Navier-Stokes equations are transformed into three recurrence relations with two independent coefficients. The boundary conditions on the cylinder's surface are satisfied in a trivial way, and the conditions at infinity lead to a system of two non linear ordinary differential equations. These are solved using Fourier series in the angular variable and, for the sake of argument, in a power series in R_e . Results on the convergence of the series, with varying order of truncation, and comparison with earlier results are discussed.

Keywords: low Reynolds number; stationary Navier-Stokes eqn's; slow viscous flow; series truncation; flow past a cylinder; drag coefficient.

Se propone un método de soluciones en series, que se truncan para obtener soluciones aproximadas al problema del flujo alrededor de un cilindro. El procedimiento está basado en una transformación en la coordenada radial, de manera que la nueva variable (x) queda definida en un intervalo finito. Las soluciones en series de potencias en x , dan pie a tres relaciones de recurrencia entre sus coeficientes, de los cuales, sólo dos son independientes. Las condiciones de frontera sobre el cilindro se satisfacen de manera trivial y la condición al infinito resulta en un sistema de dos ecuaciones diferenciales ordinarias no lineales. Estas últimas se resuelven usando series de Fourier, en la variable angular, y series de potencias en R_e ; esto con el fin de estudiar algunas características generales. Se discuten los resultados al variar el orden en el que se truncan las series y se comparan con resultados conocidos.

Descriptores: Número de Reynolds bajo; Eqs. de Navier-Stokes estacionarias; flujo viscoso y lento; truncamiento de series; flujo alrededor de un cilindro; coeficiente de arrastre.

PACS: 47.15.GF

1. Introduction

The steady viscous flow past a fixed cylinder is perhaps the simplest classical nontrivial problem in fluid dynamics. When Stokes formulated the general equations for what are now called Newtonian fluids, he addressed this problem, together with its three-dimensional analog, the problem of the flow past a sphere [1]. He was unable to find a solution and its full understanding is still the subject of analytical research, in spite of the undeniable value of numerical solutions [2–5].

In this work the power series solution method is applied to the problem of a steady viscous flow past a fixed circular cylinder. This approach to solving differential equations dates back to Newton, and is still the most commonly used and successful procedure. Here, we analyze the full Navier-Stokes equations to study the advantages of suitably built series over other different approximations made throughout the years [6–9].

Phenomenologically, this flow presents different regimes depending on the value of the Reynolds number (R_e), defined here in terms of the cylinder's radius, a . As R_e is steadily increased from some initial small value, the lack of fore and aft symmetry slowly becomes apparent, until a value close to 2.5 is reached. Afterwards, difficult to resolve at first, a recirculating region develops on the wake, and attached to the cylinder. Within this region, two standing eddies evolve until the flow, for $R_e \sim 10$, ceases to remain steady, as the eddies detach alternatively and travel down the wake giving rise to a periodic flow [10, 11]. That is, the velocity and pressure fields are time independent provided $R_e \leq 10$.

This problem has been studied for the past 150 years, and a solution is yet to be found. Even for $R_e \ll 1$, the problem displays a singular nature, as regular perturbation theory becomes singular. That is, it is not possible to find an approximation for the velocity and pressure fields, as a power series in R_e , consistent with the governing equations and the appropriate boundary conditions; this is known as Stokes' paradox. In 1910, Oseen [6, 10] pointed out that for the three-dimensional case, where a zeroth order solution exists and the first order correction cannot be found, the neglected terms are not everywhere small, and proposed an alternative way to linearize the Navier-Stokes equations. The resulting equations were solved analytically [12], for $R_e \ll 1$, but provided no systematic way or indication as to how to improve the approximation.

The first numerical calculations were performed in the late 1930's, for fixed values of R_e [13]. In the 1950's the method of matched asymptotic expansions was proposed [8, 14, 15], and applied to this problem a few years later [7, 16, 17]. The basic idea of this method is to build consistent expressions near and far from the body, the inner and outer regions, and devise an adequate procedure for matching successive approximations. The difficulty with this method is that, in order to obtain valid solutions for $R_e \sim 1$, an infinite number of corrections need to be calculated [10, 17]. To this day, many different numerical [2–4, 18–22] and analytical studies [9, 23] have been carried out for this problem.

Here, the power series solution method is used on a transformed radial variable, defined in such a way that its domain ranges between 0 and 1 and follows a previous, unpublished

work [24]. The nonlinear partial differential equations are then mapped into a set of three recurrence relations, for the coefficients of the power series; all coefficients can be written in terms of two unknown functions of the angular variable and R_e . The boundary conditions on the cylinder's surface are satisfied trivially. The uniform flow condition at infinity leads to a set of two non-linear ordinary differential equations, of infinite order and degree. To proceed further, the power series is truncated at some order N , and the corresponding pair of equations is then solved analytically. This is done for increasingly larger values of N , and with various degrees of approximation using Mathematica.

In Sec. 2, the general problem is formulated and the procedure is described. Section 3 includes the proper calculations, using Fourier series for the angular variable and, for the sake of explicit expressions, a power series in R_e is introduced. Section 4 present some results, a discussion on convergence, and some perspectives for future analyzes within this framework. The appendix illustrates the method as an example for the simplest non-trivial case and the numerical procedure is discussed.

2. Problem and procedure

The problem of the steady viscous flow around a fixed circular cylinder is described by the following system of dimensionless partial differential equations:

$$R_e(\vec{u} \cdot \nabla)\vec{u} = -\nabla P + \nabla^2 \vec{u}, \tag{1}$$

$$\nabla \cdot \vec{u} = 0; \tag{2}$$

where $\vec{u} = \vec{u}(r, \theta)$ and $P = P(r, \theta)$ are the velocity and pressure fields, r and θ are the radial and angular cylindrical coordinates, and $R_e = aU/\nu$ is the Reynolds number, U and ν being the velocity at infinity and the kinematic viscosity coefficient, respectively. The boundary conditions correspond to the stick boundary condition on the surface of the cylinder and a uniform flow with constant pressure far away from the cylinder:

$$\vec{u} = 0 \text{ if } r = 1, \tag{3}$$

$$\vec{u} = \hat{U} \text{ and,} \tag{4}$$

$$P^* \rightarrow 0 \text{ if } r \rightarrow \infty, \tag{5}$$

where \hat{U} is a unitary vector in the direction of the uniform flow, $P^* = P - P_0$, P_0 is the pressure at infinity. Equations (1) and (2) establish the conservation of momentum and mass [25–27]. The density and temperature, and hence the internal energy, are assumed to be constant over the entire domain; a common assumption, though debatable.

The first issue is that, taking into account that the region of non uniformity is in the neighborhood of the point at infinity or, equivalently, that the singular character of a straightforward perturbation theory arises from the nature of the infinite domain [10], a new variable may be introduced that is everywhere finite. Here we follow closely a previous, unpublished

paper [24]. Let

$$x(r) = 1 - \frac{1}{r}, \tag{6}$$

so that the interval $[1, \infty)$ is mapped into the interval $[0, 1]$. The Navier-Stokes equations (1) and (2), in cylindrical coordinates, now read

$$R_e \left[(1-x)u_x \frac{\partial u_x}{\partial x} + u_\theta \frac{\partial u_x}{\partial \theta} - u_\theta^2 \right] = - (1-x) \frac{\partial P^*}{\partial x} + (1-x)^3 \frac{\partial^2 u_x}{\partial x^2} + (1-x) \frac{\partial^2 u_x}{\partial \theta^2} - (1-x)^2 \frac{\partial u_x}{\partial x} - 2(1-x)u_x, \tag{7}$$

$$R_e \left[(1-x)u_x \frac{\partial u_\theta}{\partial x} + u_\theta \frac{\partial u_\theta}{\partial \theta} + u_x u_\theta \right] = - \frac{\partial P^*}{\partial \theta} + (1-x)^3 \frac{\partial^2 u_\theta}{\partial x^2} + (1-x) \frac{\partial^2 u_\theta}{\partial \theta^2} - (1-x)^2 \frac{\partial u_\theta}{\partial x} + 2(1-x) \frac{\partial u_x}{\partial \theta} - (1-x)u_\theta, \tag{8}$$

$$(1-x) \frac{\partial u_x}{\partial x} + \frac{\partial u_\theta}{\partial \theta} + u_x = 0, \tag{9}$$

Clearly, the boundary conditions in the new set of variables (x, θ) are

$$u_x(0, \theta) = 0, \tag{10}$$

$$u_\theta(0, \theta) = 0, \tag{11}$$

$$u_x(1, \theta) = \cos \theta, \tag{12}$$

$$u_\theta(1, \theta) = -\sin \theta, \tag{13}$$

$$P^*(1, \theta) \rightarrow 0, \tag{14}$$

where equations (10) and (11) correspond to the non-slip boundary condition on the cylinder's surface ($x = 0$), and equations (12), (13), and (14) are the conditions of uniform flow field and constant pressure at infinity.

The solutions for the velocity and pressure fields are assumed to have the form

$$u_x(x, \theta; R_e) = \sum_{n=0}^{\infty} a_n(\theta; R_e)x^n, \tag{15}$$

$$u_\theta(x, \theta; R_e) = \sum_{n=0}^{\infty} b_n(\theta; R_e)x^n, \tag{16}$$

$$P^*(x, \theta; R_e) = \sum_{n=0}^{\infty} c_n(\theta; R_e)x^n, \tag{17}$$

where the coefficients a_n , b_n and c_n must to be periodic, with period 2π . To satisfy conditions (10) and (11), it suffices to set the coefficients a_0 and b_0 equal to zero.

Substituting expressions (15-17) into equations (7-9), and collecting equal powers of x , results in a set of three coupled recurrence relations:

$$a_n = \frac{1}{n} [(n - 2)a_{n-1} - b'_{n-1}], \tag{18}$$

$$b_n = \frac{1}{n(n - 1)} \left\{ 2a'_{n-3} - 2a'_{n-2} + b''_{n-3} - b''_{n-2} + (n - 2)(n - 4)b_{n-3} - (3n^2 - 13n + 13)b_{n-2} + (3n - 5)(n - 1)b_{n-1} + c'_{n-2} + R_e \sum_{m=1}^{n-3} b_m [b'_{n-m-2} - (m - 1)a_{n-m-2} + ma_{n-m-1}] \right\}, \tag{19}$$

$$c_n = \frac{1}{n} \left\{ -a''_{n-2} + a''_{n-1} - (n - 1)(n - 3)a_{n-2} + (3n^2 - 7n + 3)a_{n-1} - n(n - 3)a_n + n(n + 1)a_{n+1} + 2b'_{n-2} - 2b'_{n-1} + (n - 1)c_{n-1} + R_e \sum_{m=1}^{n-2} [b_m(b_{n-m-1} - a'_{n-m-1}) + ma_m(a_{n-m-1} - a_{n-m})] \right\}, \tag{20}$$

where the primes denote derivatives with respect to θ ; these relations are valid for $n > 0$. Computing the first few coefficients, it is readily found that there are only two independent coefficients, $c_0(\theta; R_e)$ and $b_1(\theta; R_e)$, hereafter denoted by $\varphi(\theta; R_e)$ and $\eta(\theta; R_e)$, respectively. The first coefficients, in terms of the two unknown functions, are

$$\begin{aligned} c_0(\theta) &\equiv \varphi(\theta), \\ a_1(\theta) &= 0, \\ b_1(\theta) &\equiv \eta(\theta), \\ c_1(\theta) &= -\eta', \\ a_2(\theta) &= -\frac{1}{2}\eta', \\ b_2(\theta) &= \frac{1}{2}[\eta + \varphi'], \\ c_2(\theta) &= -\frac{1}{2}[\eta' + \varphi''], \\ a_3(\theta) &= -\frac{1}{3!}[2\eta' + \varphi''], \\ b_3(\theta) &= -\frac{1}{3!}[2\eta'' - 3\eta - 4\varphi'], \\ c_3(\theta) &= \frac{1}{3!}[\eta''' - 2\eta' - 3\varphi'' + 2R_e\eta^2], \\ a_4(\theta) &= \frac{1}{4!}[2\eta''' - 7\eta' - 6\varphi''], \\ b_4(\theta) &= -\frac{1}{4!}[12\eta'' - 12\eta + 2\varphi''' - 19\varphi' - R_e\eta\eta'], \\ c_4(\theta) &= \frac{1}{4!}[6\eta''' - 6\eta' + \varphi^{(4)} - 11\varphi'' + R_e(6\eta\varphi' + 2\eta\eta'' - 4\eta'^2 + 12\eta^2)]; \end{aligned}$$

the dependence on R_e has been omitted. After expressions (15) and (16) are substituted into the boundary conditions (12) and (13), they become

$$\sum_{n=1}^N a_n(\theta; R_e) = \cos \theta, \tag{21}$$

$$\sum_{n=1}^N b_n(\theta; R_e) = -\sin \theta, \tag{22}$$

for $N \rightarrow \infty$.

When the coefficients a_n, b_n and c_n are expressed in terms of $\varphi(\theta)$ and $\eta(\theta)$, the above expressions correspond to two non-linear ordinary differential equations. In order to have symmetric solutions, with respect to the transformation $\theta \rightarrow -\theta$, i.e. the velocity field on the horizontal axis must be radial, the angular component of the velocity field must be zero at $\theta = 0$ and $\theta = \pi$, which implies that $b_n(0) = b_n(\pi) = 0$. Therefore, from relations (18-20) it follows that the functions η and φ have to satisfy equations (21) and (22) with the subsidiary conditions

$$\varphi^{(2n+1)}(0) = \varphi^{(2n+1)}(\pi) = 0, \tag{23}$$

$$\eta^{(2n)}(0) = \eta^{(2n)}(\pi) = 0, \tag{24}$$

$$n = 0, 1, 2, \dots$$

Since the coefficients a_n and b_n depend only on $\eta(\theta), \varphi'(\theta)$ and higher derivatives, then, to find $\varphi(\theta)$, condition (14) must be used.

To go any further, the series (15-17) must be truncated at some fixed value N . Hence, expressions (21) and (22) yield a system of two equations for $\eta(\theta)$ and $\varphi'(\theta)$, whose order and degree depend on N . As N is increased, it is expected to that the solutions converge to the solutions of the original equations. This is yet to be proven, although the solutions found for the values of N considered here seem to behave accordingly.

2.1. The Truncated Equations

For example, expressions (21) and (22) truncated at $N = 4$ read

$$2\eta''' - 10\varphi'' - 27\eta' = 24 \cos \theta, \quad (25)$$

$$2\varphi''' - 47\varphi' + 20\eta'' - 60\eta - R_e\eta'\eta = 24 \sin \theta, \quad (26)$$

which is the first nonlinear problem to be solved. For $N = 5$ the equations are

$$2\varphi^{(4)} + 28\eta''' - 87\varphi'' - 168\eta' - R_e[\eta''\eta + \eta'^2] = 120 \cos \theta, \quad (27)$$

$$3\eta^{(4)} - 32\varphi''' - 178\eta'' + 342\varphi' + 360\eta + R_e[20\eta'\eta + 2\varphi''\eta] = -120 \sin \theta. \quad (28)$$

Clearly, the complexity of the differential equations increases rapidly with N ; the order increases as $N - 1$, while the variation of the degree of the non-linear terms on N is not clear.

2.1.1. Fourier Series

From the symmetry properties of the ordinary differential equations for a given N , it is found that the coefficients associated with the velocity and pressure fields have the form

$$a_n(\theta; R_e) = \sum_{l=0}^{\infty} \alpha_{nl}(R_e) \cos(l\theta), \quad (29)$$

$$b_n(\theta; R_e) = \sum_{l=0}^{\infty} \zeta_{nl}(R_e) \sin(l\theta), \quad (30)$$

$$c_n(\theta; R_e) = \sum_{l=0}^{\infty} \varepsilon_{nl}(R_e) \cos(l\theta); \quad (31)$$

in practice these series must be truncated at some order M . After the substitution of the above expansions into the recurrence relations (18–20) and using the orthogonality properties of the trigonometric functions, a new set of recurrence relations is obtained for the coefficients of the series (29-31) given by

$$\alpha_{nl} = \frac{1}{n} [(n - 2)\alpha_{n-1,l} - l\zeta_{n-1,l}], \quad (32)$$

$$\zeta_{nl} = \frac{1}{n(n-1)} \left\{ 2l(\alpha_{n-2,l} - \alpha_{n-3,l}) + [(n-2)(n-4) - l^2]\zeta_{n-3,l} - [(3n^2 - 13n + 13) - l^2]\zeta_{n-2,l} + (3n-5)(n-1)\zeta_{n-1,l} - l\varepsilon_{n-2,l} + \frac{1}{2}R_e \sum_{m=1}^{n-3} \sum_{p,k=1}^M [\zeta_{mp}(k\zeta_{n-m-2,k} - (m-1)\alpha_{n-m-2,k} + m\alpha_{n-m-1,k}) \times (\delta_{p,k+l} + \delta_{p,l-k} - \delta_{p,k-l})] \right\}, \quad (33)$$

$$\varepsilon_{nl} = \frac{1}{n} \left\{ [l^2 - (n-1)(n-3)]\alpha_{n-2,l} - [l^2 - (3n^2 - 7n + 3)]\alpha_{n-1,l} - n(3n-2)\alpha_{nl} + n(n+1)\alpha_{n+1,l} - 2l(\zeta_{n-1,l} - \zeta_{n-2,l}) + (n-1)\varepsilon_{n-1,l} + R_e \sum_{m=1}^{n-2} \sum_{p,k=1}^M [\zeta_{mp}(\zeta_{n-m-1,k} + k\alpha_{n-m-1,k})(\delta_{p,k+l} + \delta_{p,k-l} - \delta_{p,l-k}) + m\alpha_{mp}(\alpha_{n-m-1,k} - \alpha_{n-m,k})(\delta_{p,k+l} + \delta_{p,k-l} + \delta_{p,l-k})] \right\}, \quad (34)$$

$$\alpha_{n0} = \zeta_{0l} = \alpha_{0l} = 0, \quad (35)$$

which are valid for $n = 1, \dots, N$ and $l = 1, \dots, M$, where δ_{nm} is the Kronecker delta. The recurrence relations (32-34) have $2M$ independent functions of R_e (ζ_{1l} and ε_{0l}), which are the coefficients of the expansions for the functions $\eta(\theta)$ and $\varphi(\theta)$.

From Eqs. (21) and (22) the corresponding boundary conditions determining the value of the coefficients ζ_{nl} and ε_{nl} are

$$\sum_{n=1}^N \alpha_{nl} = \delta_{1l}, \quad (36)$$

$$\sum_{n=1}^N \zeta_{nl} = -\delta_{1l}. \quad (37)$$

With relations (32–34), the coefficients ζ_{nl} and ε_{nl} can be computed in terms of the independent coefficients ζ_{1l} and ε_{0l} . Thus, Eqs. (36) and (37) result in a system of $2M$ non-linear algebraic equations for $2M$ unknown functions of R_e (see Appendix A). Although the non-linear partial differential equations have been reduced to solve a system of algebraic equations, the problem is still non-linear.

2.1.2. The Algebraic Equations

The complexity of Eqs. (36) and (37) depends on the values of N and M and, in general, they cannot be solved analytically; an approximate solution is proposed as follows. A first attempt to solve them is to assume that the unknown coefficients have expansions in powers of R_e , i.e.

$$\zeta_{1l}(R_e) = \sum_{j=0}^{M'} \omega_{1lj} R_e^j, \tag{38}$$

$$\varepsilon_{0l}(R_e) = \sum_{j=0}^{M'} \gamma_{0lj} R_e^j, \tag{39}$$

where the coefficients ω_{1lj} and γ_{0lj} are pure numbers and $l = 1, 2, \dots, M$. In principle, the sums in the above series run up to infinity, but in order to find solutions these series must be truncated at some power M' . Substituting expressions (38) and (39) into Eqs. (36) and (37), written in terms of the $2M$ independent coefficients, and collecting terms in powers of R_e , the problem reduces to a complete system of $2M$ linear algebraic equations which can be solved iteratively. Therefore, in order to have solutions up to an order M' in R_e , M' systems of $2M$ linear equations need to be solved.

To simplify the iterative method for finding approximate solutions for Eqs. (36) and (37) using power series in R_e , one assumes that the Fourier coefficients α_{nl} , ζ_{nl} and ε_{nl} have the following expansions:

$$\alpha_{nl}(R_e) = \sum_{j=0}^{M'} \mu_{nlj} R_e^j, \tag{40}$$

$$\zeta_{nl}(R_e) = \sum_{j=0}^{M'} \omega_{nlj} R_e^j, \tag{41}$$

$$\varepsilon_{nl}(R_e) = \sum_{j=0}^{M'} \gamma_{nlj} R_e^j, \tag{42}$$

and thus the recurrence relations (32-34) can be written in terms of these coefficients; after collecting terms in powers of R_e , a new set of recurrence relations for the coefficients of the power series (40-42) is obtained. In this case, the independent coefficients are ω_{1lj} and γ_{0lj} ; given this set of numbers, all the remaining coefficients can be computed. The above expressions were truncated in order to have relations with a finite number of terms, otherwise the recurrence relations involve infinite sums.

When expressions (40-42) are substituted into conditions (36) and (37), and terms with the same power on R_e

are collected, the following relations are found

$$\sum_{n=1}^N \mu_{nlj} = \delta_{0j} \delta_{1l}, \tag{43}$$

$$\sum_{n=1}^N \omega_{nlj} = -\delta_{0j} \delta_{1l}, \tag{44}$$

so that, for fixed values of j and expressing the coefficients μ_{nlj} and ω_{nlj} in terms of the independent coefficients ω_{1lj} and γ_{0lj} , the above expressions result in a complete system of $2M$ linear algebraic equations. These equations can be solved in an iterative manner, though the calculations can be very large depending on the values of M and M' . Hence, the approximate solutions of (21) and (22) are

$$\eta(\theta; R_e) = \sum_{l=1}^M \sin(l\theta) \sum_{j=0}^{M'} \omega_{1lj} R_e^j, \tag{45}$$

$$\varphi(\theta; R_e) = \sum_{l=1}^M \cos(l\theta) \sum_{j=0}^{M'} \gamma_{0lj} R_e^j. \tag{46}$$

Equations (36) and (37) were also solved numerically for fixed values of R_e . The numerical calculations were made using Mathematica 4.0, which uses Newton's method, for different values of M and N .

2.2. Numerical Solution

In order to study the validity of the approximate solutions (45) and (46), the system of equations given by (21-24) was solved numerically for a few fixed values of N and R_e . The method used to make the numerical integration was to transform the set of boundary conditions (23) and (24) onto a set of initial conditions, which is described in Appendix B. The initial value problem was then solved in Mathematica 4.0, based on an algorithm that uses a Runge-Kutta method.

2.3. Stream Function and Drag

Once the coefficients ζ_{1l} and ε_{1l} are known for fixed values of N and M , the coefficients $\alpha_{nl}(R_e)$, $\zeta_{nl}(R_e)$ and $\varepsilon_{nl}(R_e)$ can be computed; thus

$$u_x(x, \theta, R_e) = \sum_{n=1}^N \left(\sum_{l=1}^M \alpha_{nl}(R_e) \cos(l\theta) \right) x^n, \tag{47}$$

$$u_\theta(x, \theta, R_e) = \sum_{n=1}^N \left(\sum_{l=1}^M \zeta_{nl}(R_e) \sin(l\theta) \right) x^n, \tag{48}$$

$$P^*(x, \theta, R_e) = \sum_{n=0}^N \left(\sum_{l=0}^M \varepsilon_{nl}(R_e) \cos(l\theta) \right) x^n. \tag{49}$$

In the case of the pressure field, the condition at infinity is not exactly satisfied at any order N , unless $N \rightarrow \infty$. The coefficients α_{nl} , ζ_{nl} and ε_{nl} are given by expressions (40-42).

The stream function, in cylindrical coordinates, is defined by

$$u_r = \frac{1}{r} \frac{\partial \Psi}{\partial \theta},$$

$$u_\theta = -\frac{\partial \Psi}{\partial r}.$$

Using the approximate solutions (47) and (48) for the velocity field, the stream function has the form

$$\Psi(r, \theta) = \sum_{n=1}^N \left(1 - \frac{1}{r}\right)^{n_r} \left(\sum_{l=1}^M \frac{\alpha_{nl}(R_e)}{l} \sin(l\theta) \right), \quad (50)$$

where the coefficients α_{nl} are given by (40).

The force on the cylinder's surface is calculated using

$$\vec{F} = \int_S \tilde{\tau} \cdot \hat{n} dS,$$

where $\tilde{\tau}$ is the stress tensor and \hat{n} is a unitary vector normal to the cylinder's surface (S). Due to the assumed symmetry of the problem, the direction of the force is the same as the direction of the uniform flow, far from the body. Thus

$$F = \int_S (\tau_{rr} \cos \theta - \tau_{r\theta} \sin \theta) dS, \quad (51)$$

where the components of the stress tensor are evaluated at the cylinder's surface, and are given by

$$\tau_{rr} = -\varphi(\theta; R_e), \quad (52)$$

$$\tau_{r\theta} = \eta(\theta; R_e); \quad (53)$$

the functions $\varphi(\theta; R_e)$ and $\eta(\theta; R_e)$ are thus the dimensionless pressure and the shear stress $\tau_{r\theta}$ on the cylinder's surface, respectively. Hereafter, we write the drag coefficient ($C_D = F/\rho U^2 a$) instead of the drag itself. Substituting expressions (45), and (46) into expression (51) and integrating over the cylinder's surface, it is found that

$$C_D = -\frac{\pi}{R_e} \left(\varepsilon_{01}(R_e) + \zeta_{11}(R_e) \right). \quad (54)$$

This is the drag coefficient, within this approximation.

3. Results

In this section, results for the functions $\varphi(\theta)$ and $\eta(\theta)$ for a wide range of values of N , M and M' , are presented. The solutions were compared with those obtained with numerical results for the systems of algebraic Eqs. (43) and (44), and numerical integration of Eqs. (21) and (22). Both the analytical and numerical calculations were made with Mathematica 4.0, as this program is capable of handling the equations to be solved, which are long and complicated. For example, when $N = 10$, the differential Eqs. (21) and (22) have 56 and 66 terms, respectively.

The stream function is compared with results obtained from the solution for Oseen's equation [28] and using matching asymptotic expansions [7, 8]. Once the components for the stress tensor were known, the drag coefficient was computed and some properties of convergence were analyzed. Finally, results were compared with experimental data [29, 30], and with other calculations using different methods [7, 8, 23].

3.1. Analytical Solutions

The system of linear algebraic Eqs. (43) and (44) were solved for values of N , M and M' up to 30, 21 and 30 respectively, and it is possible to go further, however, the results are only valid for $R_e < 1$, and therefore it is not useful to increase the values of M' .

The approximate solutions of (21) and (22), given N and up to $R_e^{M'}$, have the general form

$$\eta^{(N)}(\theta; R_e) = \sum_{l=1}^M \left(\sum_{j=l-1}^{M'} \omega_{1lj} R_e^j \right) \sin(l\theta), \quad (55)$$

$$\varphi^{(N)}(\theta; R_e) = \sum_{l=0}^M \left(\sum_{j=l-1}^{M'} \gamma_{0lj} R_e^j \right) \cos(l\theta), \quad (56)$$

$$\omega_{nlj} = \gamma_{nlj} = 0, \text{ for } l \text{ and } j \text{ both even or odd,}$$

where the superscript N denotes the order of truncation. These solutions show that, if the series in powers of R_e are truncated so that that $M' < M$, then the coefficients of the Fourier series (29-31), for $l > M' + 1$, are all equal zero. In other words, the Fourier series are automatically truncated such that $M = M' + 1$. Therefore, solutions provided by (55) and (56) are approximations, up to terms of order M' in R_e , of equations (43) and (44) in the limit $M \rightarrow \infty$. On the other hand, if $M < M'$, the results obtained are solutions of Eqs. (43) and (44) in the limit $M' \rightarrow \infty$. Preliminary results show that the Fourier series converge faster than the power series, i.e, the best way to truncate both series is choosing $M < M'$.

Expressions (55) and (56) are plotted in Figs. 1 and 2 for different values of R_e and N , with $M = 21$ and $M' = 30$, that is 21 terms in Fourier series and 30 powers in R_e . It can be seen that, for $R_e < 1$, the differences between solutions with increasing values of N decrease; when R_e is of order one, the convergence of the solutions, as function of N , is ill-behaved. It is clear that the asymmetry in the curves increases as N is increased, which means that the for and aft asymmetry is apparent, even for $R_e \ll 1$. Clearly, as R_e is increased with fixed N , the asymmetry increases too.

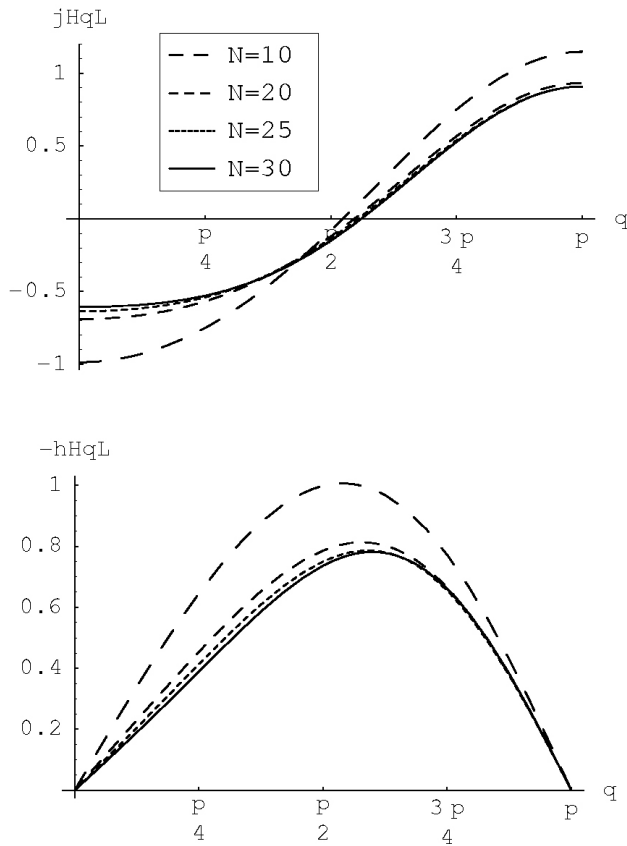


FIGURE 1. Plots of $\varphi^{(N)}(\theta)$ and $\eta^{(N)}(\theta)$ for $Re = 0.5$.

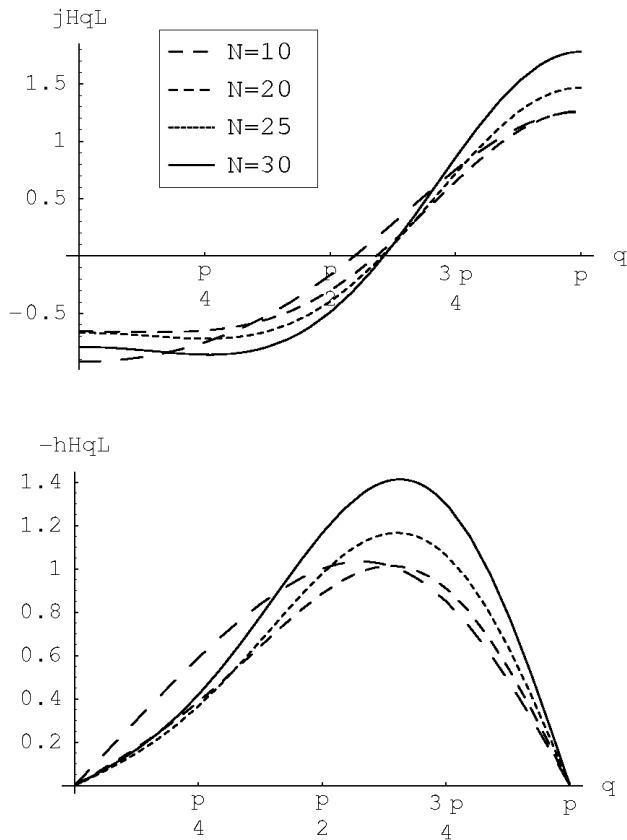


FIGURE 2. Plots of $\varphi^{(N)}(\theta)$ and $\eta^{(N)}(\theta)$ for $Re = 1$.

From the two sets of functions $\{\eta^{(N)}(\theta; Re)\}$ and $\{\varphi^{(N)}(\theta; Re)\}$, the stream lines can be calculated using expression (50). Some are plotted in Fig. 3 for different values of N and Re . It is clear how the asymmetry increases, between up and down stream regions, as N is increased with fixed Re and vice-versa.

The results for the stream lines, calculated using this method, were compared with results obtained using Oseen's equation and matching asymptotic expansions. Solutions for the stream function, found by Lamb [10, 12, 28], by Kaplun [8, 10] and with this method for $N = 30$, are shown in Fig. 4. For $Re < 0.5$, larger differences are observed between $N = 30$ and the Oseen approximation, hence, our results are in good agreement with the fact that Kaplun's solution is a better approximation than Lamb's approximate solution. It may be seen too, that the differences between solutions for the stream lines increase far from the cylinder. However, solutions corresponding to other calculations are only valid

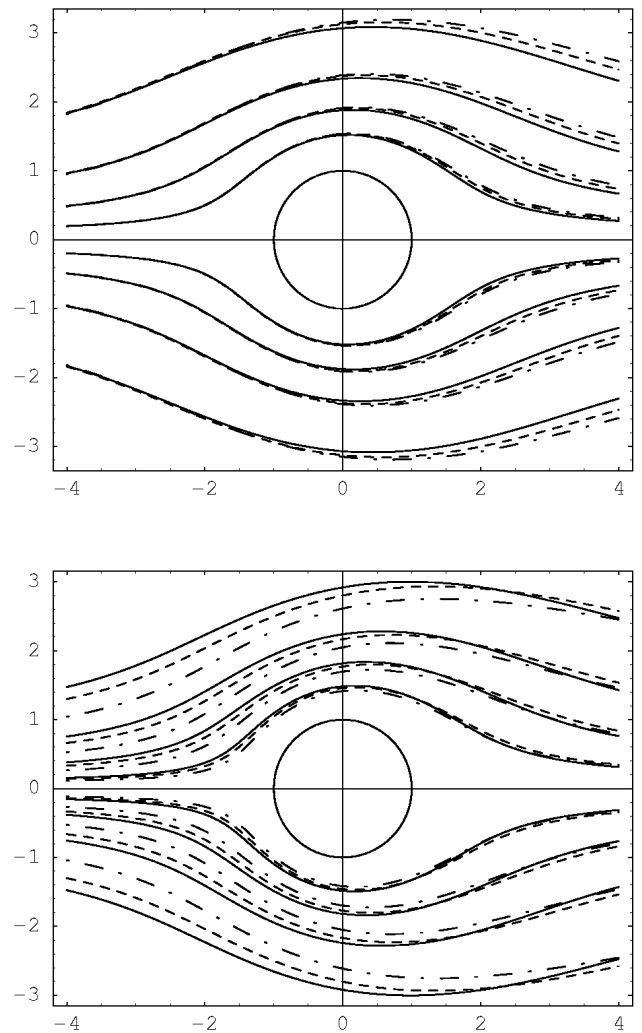


FIGURE 3. Stream lines for $Re = 0.5$ (top) and $Re = 1$ (bottom) for $N = 20$ (continuous), $N = 25$ (dashed) and $N = 30$ (dashed-dot). The flow is from left to right.

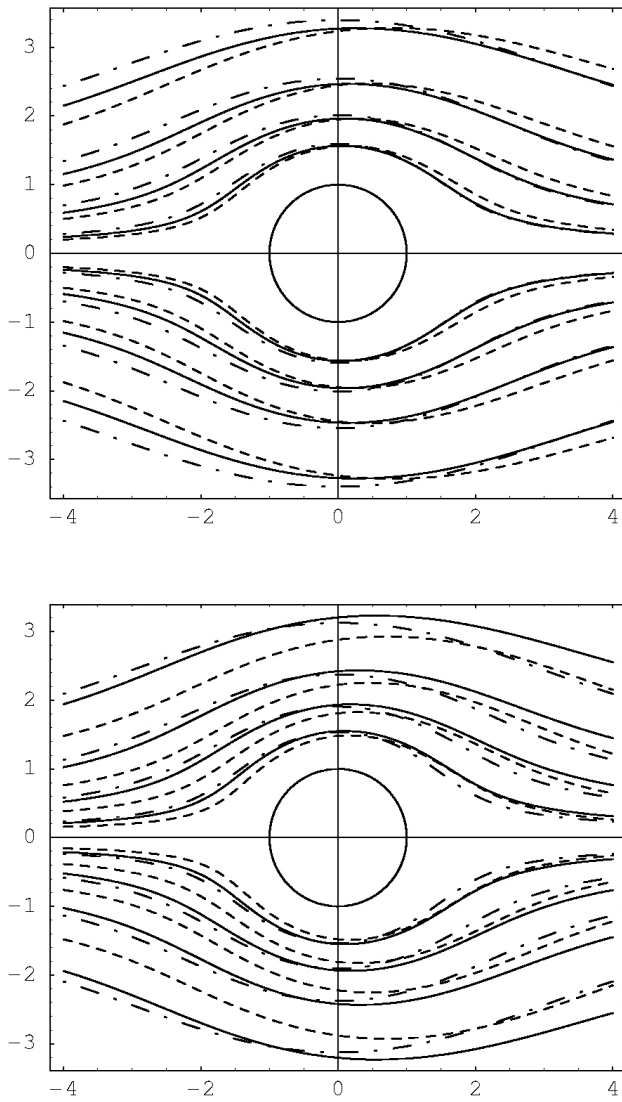


FIGURE 4. Stream lines for $R_e = 0.2$ (top) and $R_e = 0.4$ (bottom) for $N = 30$ (continuous), Oseen approximation (dashed) and matched asymptotic expansions (dashed-dot).

when $R_e r \ll 1$, where r is the usual radial coordinate, and for the present calculations, the solutions are valid for $x \ll 1$.

In the case of the drag coefficient, combining expressions (40-42) with (54), it follows that

$$C_D^{(N)} = -\frac{\pi}{R_e} \sum_{j=0}^{M'} (\omega_{11j} + \gamma_{01j}) R_e^j. \quad (57)$$

In Figs. 5 and 6, expression (57) is plotted for different values of N , and with the earlier results of Lamb [12], Kaplun [8], and the experimental results of Tritton [30] and Huner and Hussey [29]. The differences between $C_D^{(N-1)}$ and $C_D^{(N)}$ diminishes as N increases, when $R_e < 1$; for values of order one, the drag coefficient increases for large values of N . Therefore, as N increases, $C_D^{(N)}(R_e)$ improves within a finite range of R_e . The asymptotic behavior of this decrease shows that if $R_e < 1$, the solutions found for a finite N seem

to converge to the solution for $N \rightarrow \infty$. The results found using this method seem to be in good agreement with those found solving Oseen's equation [12], matching asymptotic expansions [7, 8, 10] and the experimental data [29, 30]. It is seen that, for a certain range of R_e , our curve seems to be a better approximation to the drag coefficient than earlier theoretical results. Kropinski *et al.* [21] obtained a result for the drag coefficient using a numerical method which is compared with the experimental results of Tritton [30] and are qualitatively similar to our results.

Table I shows a comparison between the solution for $N = 30$ and the numerical results made by Hamielec & Raal [31] and Keller & Takami [5], and the interpolated experimental data of [29, 30]. Clearly, the present results differ from these numerical and experimental results, due to the slow convergence of the power series in x .

TABLE I. Comparison for the Drag coefficient for two different values of R_e .

R_e	$N=30$	Hamielec & Raal	Keller & Takami	Tritton	Hunner & Hussey
0.5	9.37	10.97	-	10.99 ± 0.27	9.62 ± 0.10
1	7.66	6.83	6.644	7.25 ± 0.21	6.67 ± 0.06

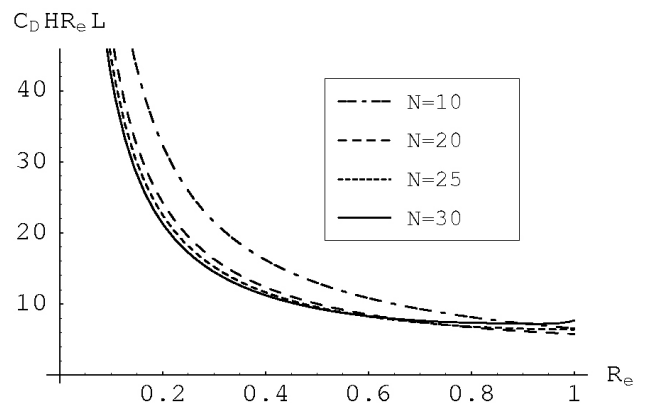


FIGURE 5. Drag coefficient as a function of R_e , for different values of N .

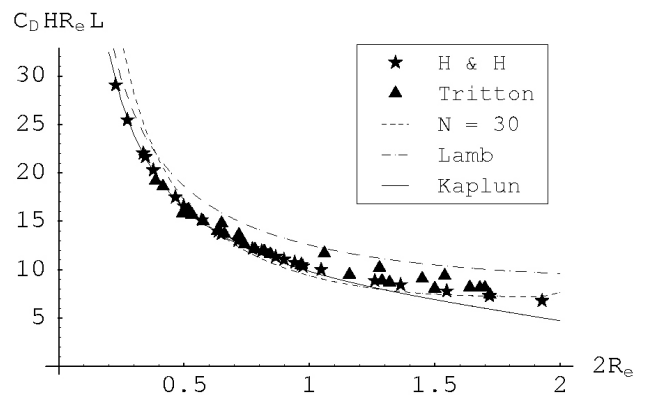


FIGURE 6. Drag coefficient.

3.2. Numerical Solutions: Results

Here a comparison between numerical results and the solutions described in the previous section is presented. Namely, between numerical and approximate analytical solutions of the system of non-linear algebraic Eqs. (36) and (37), and the system of non linear ordinary differential Eqs. (21) and (22). All the numerical calculations were made using Mathematica 4.0.

3.2.1. Algebraic Equations

In order to solve numerically the system of non-linear algebraic Eqs. (36) and (37), R_e and the index M were fixed, so a system of $2M$ non-linear equations for $2M$ unknowns is obtained. When $M = 2, 3$ and $N = 4, 5, 6$, the corresponding equations can be solved analytically for all R_e (see Appendix A). For larger values of M , the analytical solutions were not found. Thus Newton's numerical method was used to find numerical solutions of (36) and (37). The largest values of N and M that were used in the numerical calculations were 8 and 5, respectively. It is worth noting that these equations become very complicated and long, for example, for $N = 8$ the differential equations have more than 35 terms each. Thus, when the algebraic equations are computed, the number of terms increases fast due to the non linear terms.

The first few cases that can be solved analytically show that, given N and M , the Taylor series in R_e , for the Fourier coefficients α_{nl} , ζ_{nl} and ε_{nl} , are the same as those found solving equations (43) and (44). For larger values of N and M , numerical results for equations (36) and (37) show that, for a finite range of R_e , the agreement with the power series solutions is very good. Due to the non-linearity of the system of Eqs. (36) and (37) there are many solutions, depending on the degree of the polynomial equations; the analyzed cases show that only one of them is physically meaningful.

3.2.2. The Non-linear Differential Equations

A numerical integration of Eqs. (21-24) was performed, for N up to 9 and for different values of R_e , in order to study the validity and convergence properties of solutions (55) and (56).

Comparing numerical and analytical solutions, it is found that, for the first few values of N , the approximate analytical solutions (55) and (56) are good approximations for a small range of values of R_e (see Appendix B).

In the numerical calculations, the values of N were taken up to 9 and for $R_e < 2$. For larger values of N and R_e the algorithm used to perform numerical calculations fails, due to the degree and order of the differential equations. As was mentioned above, the set of boundary conditions is transformed to a set of initial conditions; thus as N increases the number of initial conditions and the degree of the differential equations increases too (see Appendix B for more details).

On the other hand, if R_e increases, the non-linear terms dominate the behavior of the solutions and the numerical method proposed does not converge.

3.3. The Asymptotic Behavior

With the solutions (55) and (56), for different values of N , M and M' , the asymptotic behavior can be analyzed. Figure 7 shows the first two Fourier coefficients of $\varphi^{(N)}(\theta)$ as functions of R_e , for different values of N . As N is increased, the difference between coefficients for consecutive values of N diminishes for small R_e ; for values of R_e of order one these differences increase. It is found too that the Fourier coefficients, for $l > 3$, increase (decrease) rapidly when R_e is of order one. Then, the convergence of series (38) and (39) is very slow with a finite convergence ratio. When the coefficients ω_{1lk} and γ_{0lk} are analyzed as functions of N , it is found that for, $l > 1$, these coefficients increase as N is increased (see Fig. 8). This behavior is due to the non-existence of solutions, in power series on R_e , for $N \rightarrow \infty$ and $R_e \rightarrow 0$. As already mentioned, it is possible to go further on the calculations for higher powers of R_e , but the results found, as functions of N , indicate that the power series representation is inadequate for R_e of order one. Therefore, no attempt was made to estimate the convergence ratio of the series (38) and (39) with more precision.

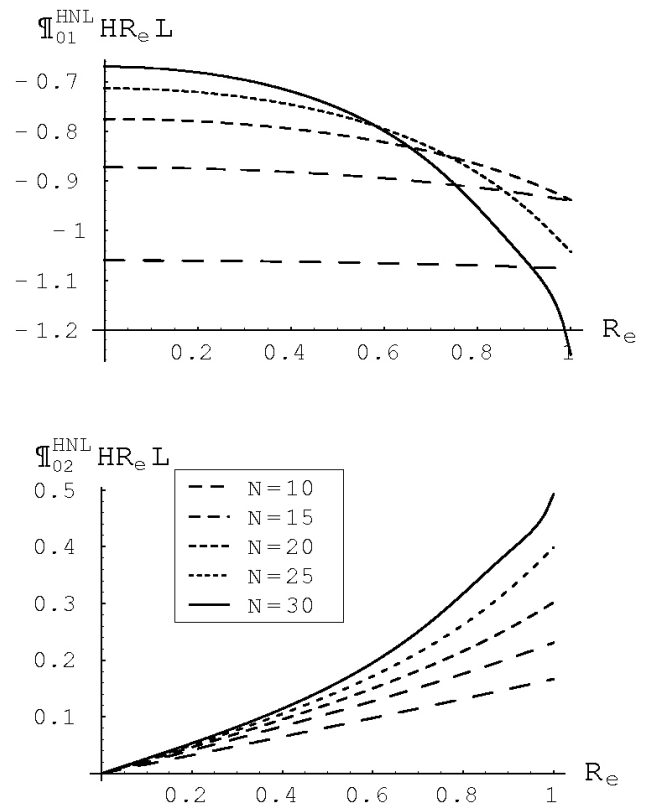


FIGURE 7. Plots of the coefficients in Eq. (39) for $l = 1$ and $l = 2$ with $M' = 30$.

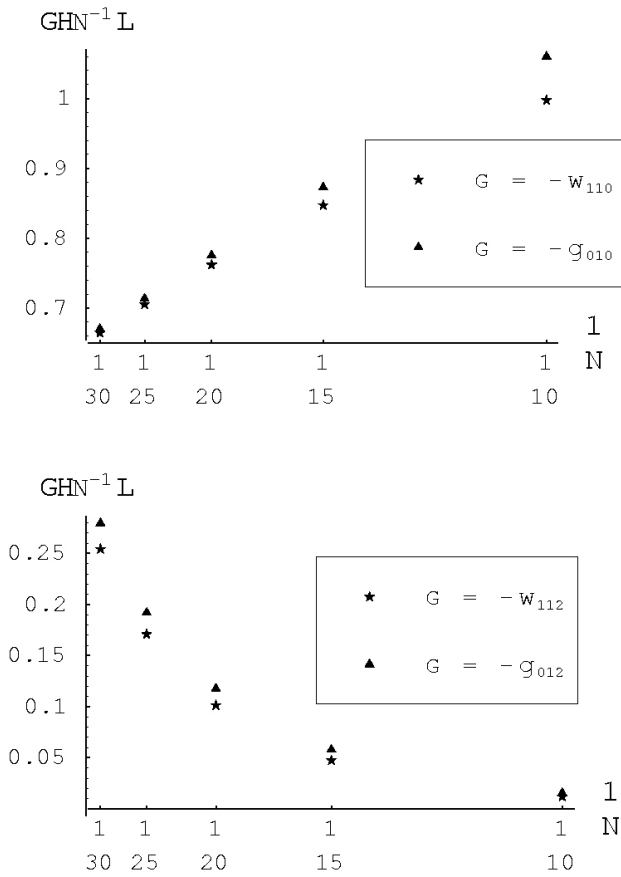


FIGURE 8. First two coefficients of the power series of Eq. (38) and (39) as functions of N .

Even when the results found show that a power series representation in R_e is ill-behaved for larger values of N , the truncated problem seems to be a fair approximation to the Navier-Stokes equations which improves when N is increased. Then, in order to find asymptotic solutions valid for R_e of order one, it is necessary to compute for larger values of N and to envisage another way of solving the system of non linear algebraic Eqs. (36) and (37), iteratively.

4. Discussion

The first advantage of this formulation is that the relevant quantities of the problem can be computed if two components of the stress tensor over the cylinder’s surface are known. That is, if $\varphi(\theta; R_e)$ and $\eta(\theta; R_e)$ are given, all the remaining features of the flow can be written as functions of them and their derivatives.

The procedure involves three independent approximations: first, by truncating the series in the new radial coordinate (fixing some value for N); second, by truncating the Fourier series in the angular variable in order to have an algebraic system involving R_e only; the third and roughest is obtained by solving the latter in powers of R_e . For small and finite R_e such representation is expected to illustrate some features of the previous two expansions.

When the series (15-17) are truncated, the approximate solutions for different values of N seem to converge slowly, as shown in Fig. 1. For a fixed value of N , and each truncation in the Fourier series, a physically meaningful solution was always found. In fact, we found solutions in power series in R_e , which are valid when the Reynolds number is small ($0 < R_e < 1$); in the simplest case ($N = 4$), and for a few cases, the calculations could be made analytically (see Appendix A) and led to rational functions in fractional powers of R_e whose Taylor series coincided with the power series representation used in Eqs. (40-42). The consequence of the non-existence of a solution to Stokes’ equations, when $R_e = 0$, is that at each order of approximation (each N) no solution satisfying the boundary conditions can be found. This is reflected in the poor estimation of the drag coefficient for $R_e \ll 1$ which seems to improve when N is increased (see Figs. 5 and 6).

Comparing the stream lines, when $R_e \ll 1$, the present results are closer to those of Kaplun [8, 10] than those using the Oseen approximation [10, 12, 28]. This might be due to the fact that both approximations are better near the cylinder. One should point out that, for a given stream line, differences in fore and aft symmetry become more apparent when N is increased, as shown in Fig. 3, as this procedure takes into account the non-linear terms at each step, through both the differential equations and the boundary conditions, as opposed to other approaches where one or the other is incorporated; and this, of course, in approximate way.

For a given N , the velocity field satisfies the Navier-Stokes equations and the boundary conditions up to order N in the radial coordinate, and order M in the Fourier series. On the other hand, the pressure field fails to satisfy the boundary condition (14) for any order. That is, one of the disadvantages of this method is that the pressure field, far from the object, does not reach a constant value as a consequence of the truncation in the power series in x . However, it is important to notice that both the velocity and pressure fields, are good approximations only in the neighborhood of the cylinder where $x \ll 1$. Comparison between our results for the pressure, $\varphi(\theta)$ in Fig. 2, and other theoretical and numerical calculations could only be carried out qualitatively, and they seem to be similar to those of Underwood [23] and Keller & Takami [5].

For the drag coefficient, as N increases, the results behave well for Reynolds numbers up to one, that is, changes are in the right direction (see Fig. 5). For $0.2 < R_e < 1$, our results are the best fit for experimental data (see Fig. 6). For Reynolds numbers larger than one, the Fourier coefficients become ill-behaved, as well as the drag. To avoid this, a more suitable representation for the dependence on the Reynolds number is required. The case $N = 4$ is still being studied in this regard. Based on the structure of the few analytical solutions that can be found, it seems that Padé approximations [32] might provide a better representation.

We emphasize that the power series in R_e cannot be used in order to find the asymptotic behavior in the limit

$N \rightarrow \infty$. In this case the problem corresponds to solving the full Navier-Stokes equations using power series in R_e , where it is known that such solutions do not exist. However, the power series representation in R_e for the truncated case shows that the power series in x , and the Fourier series in the angular variable, are suitable representations for the approximate solutions for the velocity and pressure fields.

Acknowledgments

FM wishes to thank the support of DGEP for a graduate scholarship. Grant 32248-E from CONACYT is gratefully acknowledged.

A Appendix: Solution for $N = 4$

The method described in section 2.1. is illustrated for $N = 4$, where some calculations can be performed analytically and written in a closed form. The system of non linear differential equations that is to be solved is

$$2\eta''' - 10\phi'' - 27\eta' = 24 \cos \theta, \quad (A.1)$$

$$2\phi''' - 47\phi' + 2\eta'' - 60\eta - R_e\eta'\eta = 24 \sin \theta. \quad (A.2)$$

In expressions (29-31), for the cases $M = 2, 3$ the algebraic equations (36) and (37) can be solved analytically using Mathematica 4.0; in these cases there is only one real solution. When the Taylor series of such solutions are computed, the results are the same as those solving the linear algebraic equations given by (43) and (44).

For example, when $M = 2$, the system of non-linear algebraic equations are

$$10\varepsilon_{01} - 29\zeta_{11} = 24,$$

$$4\varepsilon_{02} - 7\zeta_{12} = 0,$$

$$98\varepsilon_{01} - \zeta_{11}(160 - R_e\zeta_{12}) = 48,$$

$$280\zeta_{12} - 220\varepsilon_{02} + R_e\zeta_{11}^2 = 0,$$

and have the following solutions

$$\varepsilon_{01} = \frac{1}{10}(24 + 29\zeta_{11}), \quad (A.3)$$

$$\varepsilon_{02} = \frac{7}{4}\zeta_{12}, \quad (A.4)$$

$$\zeta_{11} = 3 \cdot 7^{1/3} \left(-\frac{69 \cdot 7^{1/3}}{R_e f(R_e)^{1/3}} + \frac{f(R_e)^{1/3}}{R_e} \right), \quad (A.5)$$

$$\zeta_{12} = \frac{3}{35} \left(-\frac{996}{R_e} + \frac{33327 \cdot 7^{1/3}}{R_e f(R_e)^{2/3}} + \frac{49^{1/3} f(R_e)^{2/3}}{R_e} \right), \quad (A.6)$$

where

$$f(R_e) = -52 R_e + \sqrt{2299563 + 2704R_e^2}.$$

These expressions have well-behaved power series expansions for $0 \leq R_e \leq 35$; just a few terms are required to

give a reasonable approximation. However, as the order of truncation is increased (N), the radius of convergence diminishes.

Though this is a simple case that does not represent a good description of the flow, it shows that the solutions to the algebraic equations can be written in terms of rational polynomials of R_e , which are regular functions at $R_e = 0$, as follows:

$$\varepsilon_{0l} = \mathcal{F}_0(R_e)\delta_{0l} + \frac{\mathcal{F}_l(R_e)}{R_e}, \quad (A.7)$$

$$\zeta_{1l} = \frac{\mathcal{G}_l(R_e)}{R_e}, \quad (A.8)$$

These expressions suggest an alternative representation for the solutions of the non linear algebraic equations.

B Appendix: Numerical Method

The procedure for transforming the system of ordinary non-linear differential equations, with boundary conditions, into an initial value problem is described for the case $N = 4$.

Writing equations (A.1) and (A.2) in terms of the function $\phi(\theta) = \varphi'(\theta)$ leads to

$$2\eta''' - 27\eta' - 10\phi' = 24 \cos \theta, \quad (B.1)$$

$$-20\eta'' + 60\eta - 2\phi'' + 47\phi + R_e\eta\eta' = -24 \sin \theta. \quad (B.2)$$

The corresponding boundary conditions are

$$\{\eta(0), \eta(\pi), \eta''(0)\} = 0, \quad (B.3)$$

$$\{\phi(0), \phi(\pi)\} = 0. \quad (B.4)$$

The initial conditions required to solve equations (B.1) and (B.2) are

$$\{\eta(0), \eta''(0), \phi(0)\} = 0, \quad (B.5)$$

$$\eta'(0) = x, \quad (B.6)$$

$$\phi'(0) = y, \quad (B.7)$$

where x and y are constants. If the system of differential equations (B.1) and (B.2) is solved for arbitrary values of x and y , then

$$\eta(\pi) = F_1(x, y),$$

$$\phi(\pi) = F_2(x, y).$$

Therefore, in order to satisfy the boundary conditions (B.3) and (B.4) the following system of equations has to be solved

$$F_1(x, y) = 0, \quad (B.8)$$

$$F_2(x, y) = 0. \quad (B.9)$$

The solutions of these equations can readily be found by the iterative gradient method

$$\vec{r}_{n+1} = \vec{r}_n - [\text{grad}\vec{H}(\vec{r}_n)]^{-1}\vec{H}(\vec{r}_n),$$

where

$$\vec{r}_n = \begin{pmatrix} x_n \\ y_n \end{pmatrix},$$

$$\vec{H}(\vec{r}_n) = \begin{pmatrix} F_1(x_n, y_n) \\ F_2(x_n, y_n) \end{pmatrix},$$

and

$$\text{grad}\vec{H}(\vec{r}_n) = \begin{pmatrix} \frac{\partial F_1}{\partial x} & \frac{\partial F_1}{\partial y} \\ \frac{\partial F_2}{\partial x} & \frac{\partial F_2}{\partial y} \end{pmatrix}.$$

Once the initial conditions are found for different values of R_e , Eqs. (B.1) and (B.2) can be integrated using Mathematica 4.0, and the results compared with the analytical solutions. In this example the calculations can be carried out for R_e up to 30; for larger values of N , the range of accessible values of R_e drastically decreases. Figure 9 shows a comparison between expression (55) and the numerical results for three different values of both N and R_e . For fixed N , the error at $\theta = \pi$ increases with the Reynolds number. On the other hand, if N increases for fixed R_e , differences between numerical and analytical results also become larger.

For the first few values of N and for $R_e < 1$, it is possible to improve the numerical results, finding the optimal size of the grid implicit in the gradient method, and using expressions (55) and (56) as an initial guess. When either N or R_e increases, the system of equations (B.1), (B.2) and (B.5-B.7) displays a strong sensitivity to the initial conditions, and thus the iterative procedure for finding the initial conditions fails to converge; even for small values of R_e .

In the numerical case, when $N > 9$, the algorithm used by Mathematica 4.0 fails, as expressions rapidly become cumbersome. As N increases the number of terms in each differential equation increases very quickly; for example, for

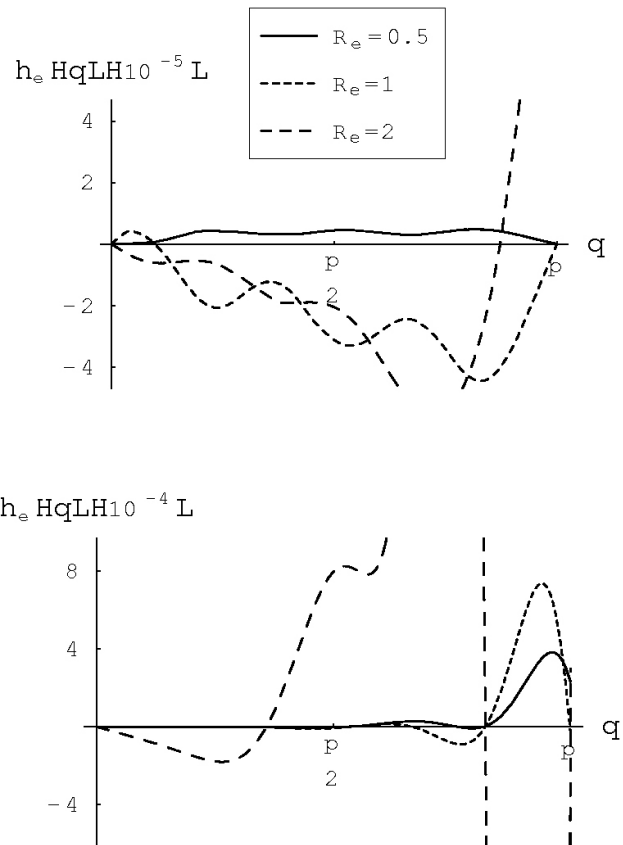


FIGURE 9. Differences between analytical result (55) and numerical results for $N = 5$ (top) and $N = 6$ (bottom).

$N = 8$ an equation has almost 40 terms, so it is difficult to handle them outside Mathematica.

Clearly, this procedure is not the most efficient way to obtain numerical solutions to the system of non-linear ordinary differential equations, for larger values of both N and R_e . But provides a reasonable idea of the validity of the analytical results, which was the basic motivation for the present case, as our interest is focused on finding and studying the functions $\eta(\theta)$ and $\varphi(\theta)$.

1. G.G. Stokes, *Trans. Camb. Phil. Soc.* **9** (1851) 8.
2. S.C.R. Dennis and G. Chang, *J. Fluid Mech.* **42** (1970) 471.
3. E.M. Saiki and S. Biringen, *J. Comput. Phys.* **123** (1996) 450.
4. K. Khadra, P. Angot, S. Parneix, and J. Caltagirone, *Int. J. Numer. Meth. Fluids* **34** (2000) 651.
5. J.B. Keller and M.J. Ward, *J. Eng. Math.* **30** (1996) 253.
6. C.W. Oseen, *Ark. Mat. Astronom. Fys.* **6** (1910).
7. I. Proudman and J.R.A. Pearson, *J. Fluid Mech.* **2**, (1957) 237.
8. S. Kaplun, *J. Math. Mech.* **6** (1957) 595.
9. S.J. Liao, *Int. J. Non-Linear Mech.* **37** (2002) 1.
10. M.V. Dyke, *Perturbation Methods in Fluid Mechanics* (Parabolic Press, 1975).
11. M. Coutanceau and R. Bouard, *J. Fluid Mech.* **79** (1977) 231.
12. H. Lamb, *Hydrodynamics*, (Dover Publications, New York, 1945), 6th ed.
13. A. Thom, *Proc. Roy. Soc. A* **141** (1933) 651.
14. P.A. Lagerstrom and J.D. Cole, *J. Rat. Mech. Anal.* **4** (1955) 817.
15. S. Kaplun and P.A. Lagerstrom, *J. Math. Mech.* **6** (1957) 585.
16. W. Chester and D.R. Breach, *J. Fluid Mech.* **37** (1969) 751.
17. L.A. Skinner, *Quart. J. Mech. Appl. Math.* **28** (1975) 333.

18. B. Fornberg, *J. Fluid Mech.* **98** (1980) 819.
19. G. Zhaoli, S. Baochang, and W. Nengchao, *J. Copm. Phys.* **165** (2000) 288.
20. X. He and G. Doolen, *J. Copm. Phys.* **134** (1997) 306.
21. M.C.A. Kropinski, M.J. Ward, and J.B. Keller, *SIAM J. Appl. Math.* **55** (1995) 1484.
22. H.B. Keller and H. Takami, in *Numerical Solutions of Non-linear Differential Equations*, edited by D. Greenspan, Wiley, 1966), Proc. of an Advanced Symp., p. 115.
23. R.L. Underwood, *J. Fluid Mech.* **37** (1969) 95.
24. R. Soto and R. Peralta-Fabi, *A power series solution to the Navier-Stokes equations for an incompressible viscous flow past a circular cylinder*, Internal Report UAM-I-F82001 (1981).
25. G.K. Batchelor, *An Introduction to Fluid Dynamics* (Cambridge University Press, 1994).
26. L.D.L. and E.M. Lifshitz, *Mecánica de Fluidos* (Reverté, 1991).
27. S. Goldstein, *Modern Developments in fluid Dynamics*, vol. 1 (Dover Publications, New York, 1965).
28. L. Rosenhead, *Laminar Boundary Layers* (Oxford University Press, London and New York, 1963).
29. B. Huner and R.G. Hussey, *Phys. Fluids* **20** (1977) 1211.
30. D.J. Tritton, *J. Fluid Mech.* **6** (1959) 547.
31. A.E. Hamielec and J.D. Raal, *Phys. Fluids* **12** (1969) 11.
32. C.M. Bender and S.A. Orszag, *Advanced Mathematical Methods For Scientists and Engineers* (Springer-Verlag, 1999).